ACS chemical biology

Articles

pubs.acs.org/acschemicalbiology

Small Molecule Microarrays Enable the Identification of a Selective, Quadruplex-Binding Inhibitor of MYC Expression

Kenneth M. Felsenstein,[†,‡,⊥,#] Lindsey B. Saunders,[§,#] John K. Simmons,[†] Elena Leon,[†,‡] David R. Calabrese,[§] Shuling Zhang,[†] Aleksandra Michalowski,[†] Peter Gareiss,[∥] Beverly A. Mock,[*,†] and John S. Schneekloth, Jr.[*,§]

[†]Laboratory of Cancer Biology and Genetics, National Cancer Institute, Building 37, Room 3146, Bethesda, Maryland 20892-4258, United States

[‡]NCI/JHU Molecular Targets and Drug Discovery Program, Baltimore, Maryland, United States

[§]Chemical Biology Laboratory, National Cancer Institute, Building 376, Room 225C, P.O. Box B, Frederick, Maryland 21702-1201, United States

[∥]Yale Center for Molecular Discovery, West Haven, Connecticut, United States

Supporting Information

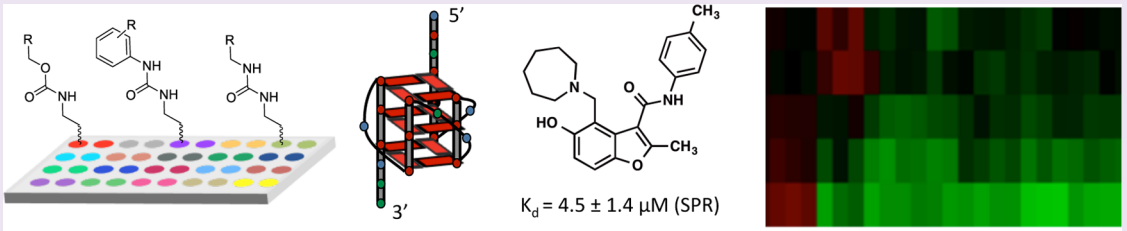

Microarray-based Discovery of Quadruplex-binding Small Molecules

ABSTRACT: The transcription factor MYC plays a pivotal role in cancer initiation, progression, and maintenance. However, it has proven difficult to develop small molecule inhibitors of MYC. One attractive route to pharmacological inhibition of MYC has been the prevention of its expression through small molecule-mediated stabilization of the G-quadruplex (G4) present in its promoter. Although molecules that bind globally to quadruplex DNA and influence gene expression are well-known, the identification of new chemical scaffolds that selectively modulate G4-driven genes remains a challenge. Here, we report an approach for the identification of G4-binding small molecules using small molecule microarrays (SMMs). We use the SMM screening platform to identify a novel G4-binding small molecule that inhibits MYC expression in cell models, with minimal impact on the expression of other G4-associated genes. Surface plasmon resonance (SPR) and thermal melt assays demonstrated that this molecule binds reversibly to the MYC G4 with single digit micromolar affinity, and with weaker or no measurable binding to other G4s. Biochemical and cell-based assays demonstrated that the compound effectively silenced MYC transcription and translation via a G4-dependent mechanism of action. The compound induced G1 arrest and was selectively toxic to MYC-driven cancer cell lines containing the G4 in the promoter but had minimal effects in peripheral blood mononucleocytes or a cell line lacking the G4 in its MYC promoter. As a measure of selectivity, gene expression analysis and qPCR experiments demonstrated that MYC and several MYC target genes were downregulated upon treatment with this compound, while the expression of several other G4-driven genes was not affected. In addition to providing a novel chemical scaffold that modulates MYC expression through G4 binding, this work suggests that the SMM screening approach may be broadly useful as an approach for the identification of new G4-binding small molecules.

The oncogenic transcription factor MYC has a pleiotropic role in a wide range of cell processes[1] and is deregulated in some 70% of human cancers.[2] However, targeting the MYC protein directly has proven to be difficult due to a lack of well-defined pockets amenable to small molecule binding,[3−6] which makes it desirable to evaluate alternative mechanisms for inhibiting MYC function.[7,8] One such mechanism is through stabilization of the G-quadruplex (G4) present in the *MYC* promoter region.[9] G4s are guanine-rich, noncanonical Hoogsteen-bonded nucleotide structures found in many RNA and DNA sequences (Figure 1A).[10,11] *MYC* Expression is regulated by a 27 base pair (Pu27) sequence, found in the nuclease hypersensitive element III(1) region ($NHEIII_1$) of the *MYC* gene, that is known to form a G4.[12] The specific mechanism by which the G4 regulates transcription remains under investigation, though one model that has been put forth is that formation of a G4 in this sequence results in a "kink" in the

Received: February 26, 2015
Accepted: October 13, 2015
Published: October 13, 2015

DOI: 10.1021/acschembio.5b00577
ACS Chem. Biol. 2016, 11, 139−148

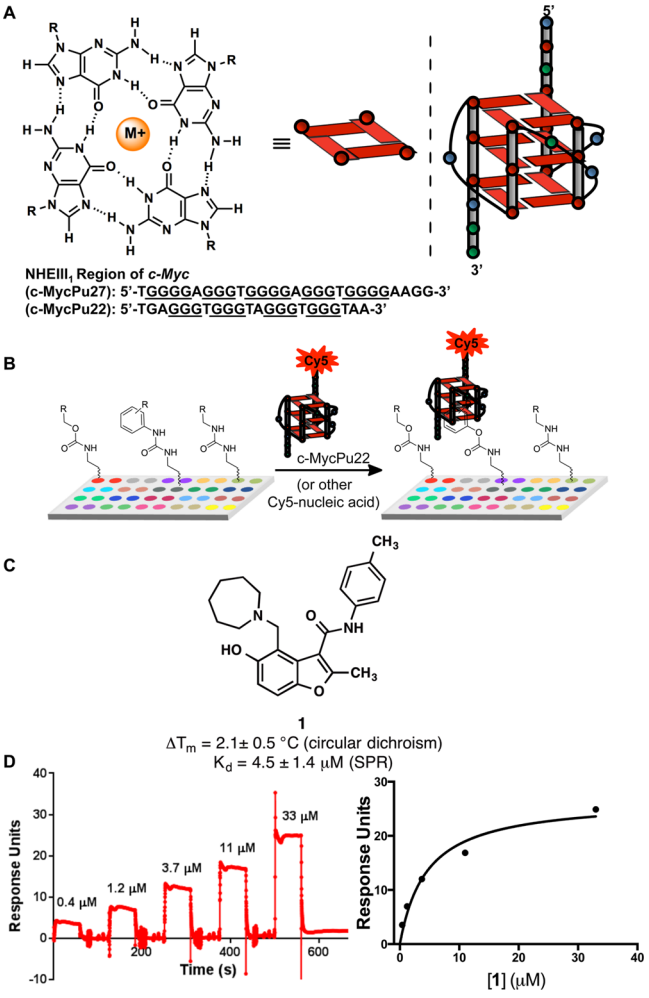

Figure 1. (A) Schematic drawing of the parallel stranded *MYC* Pu22 G4. Each colored circle represents a different nucleotide (A, green; G, red; T, blue). The G4-forming promoter sequence of the NHE III_1 region of wild type *MYC* Pu27 and variant *MYC* Pu22 are indicated. (B) Cartoon depicting a small molecule microarray screen to identify compounds that bind to *MYC* G4 DNA. (C) Structure of compound **1** identified from the SMM screen to selectively bind to *MYC* Pu22. **1** increases the melting temperature of G4 DNA as measured by circular dichroism (average of four trials ± standard deviation). (D) Surface plasmon resonance (SPR) experiment to measure the binding of **1** to *MYC* Pu22. Shown are the sensorgram (left) and binding isotherm (right). The reported K_d value is the mean of three experiments ± standard deviation.

DNA that prevents the polymerase from continuing along its reading frame, ultimately resulting in down-regulation of the associated gene.[13] A second, and perhaps more likely, model suggests that G4 formation modulates protein−DNA interactions (for example, with nucleolin[14] or ADAR1[15]), leading to regulation of transcription. The use of small molecules to stabilize the G4 conformation and consequently decrease *MYC* expression is an attractive therapeutic goal in cancers where MYC contributes to the oncogenic phenotype. Many G4 stabilizing compounds are known; however, a G4-modulating drug remains elusive. Thus, approaches to identify new G4 binders are of high interest.[16]

Previous studies have robustly demonstrated that small molecules that bind tightly to the *MYC* G4 affect MYC expression.[17] A number of reported ligands, many with nanomolar affinity, are known to effectively stabilize G4 DNA according to structural and biophysical measurements;[18,19] however, not all of these molecules have been validated in cellular models or *in vivo*.[20,21] Additionally, although some G4 ligands silence *MYC* expression in cells, many are not selective,[22] and their activity cannot always be attributed to a *MYC* G4-dependent mechanism of action.[23] The only G4-stabilizing molecule that has advanced to clinical trials is Quarfloxin (CX-3552, Cylene Pharmaceuticals, Tetragene), which induces apoptosis and cell death in cancer cells. Its mechanism of action is believed to involve the inhibition of rRNA biogenesis via disruption of the interaction between nucleolin and ribosomal G4 DNA.[24] Furthermore, many other reported G4 ligands are also duplex DNA intercalators, exhibit promiscuous reactivity, or bind to G4s with greater than a 1:1 binding stoichiometry.[9,25,26] TMPyP4, a commonly used reagent in G4 binding studies, is a cationic porphyrin that binds G4 DNA in multiple fashions[27] and exhibits significant off-target activity.[28−30] A second prominent example is pyridostatin, which was designed to bind all G4s in the cell.[31,32] Another notable G4-stabilizing molecule is BRACO-19, comprised of an acridine scaffold.[33−35] New structural classes of potent, selective G4 ligands that selectively silence genes by stabilizing G4 DNA are of substantial utility as reagents to study *MYC* biology, to understand quadruplex-dependent gene regulation, and as potential scaffolds for therapeutic development. The continued emergence of G4s as regulatory elements in many genes means that new methods to rapidly identify novel G4 binding small molecule scaffolds with differential binding profiles are also of high importance.

Here, we report an approach for the identification and characterization of a new class of small molecule *MYC* G4 ligands using small molecule microarrays (SMMs). Although SMMs have been broadly used to identify inhibitors of protein targets, they have been used much less often for nucleic acid structures. We hypothesized that using an unbiased SMM screen might provide a rapid method for the identification of new quadruplex-binding molecules. To realize this goal, we performed a SMM screen of 20 000 compounds using a fluorescently tagged G4 DNA oligonucleotide derived from the $NHEIII_1$ region in the *MYC* promoter.[12] One of the small molecules identified in this screen, compound **1**, inhibits *MYC* transcription *in vitro* in a G4-dependent fashion. Direct and reversible binding to *MYC* G4-DNA was validated through SPR and thermal melt assays. Furthermore, decreased *MYC* transcription correlated with decreased viability across a panel of multiple myeloma cell lines. In addition, the compound has minimal effect on cell viability in a Burkitt's lymphoma cell line harboring a *MYC* translocation that deletes the G4 in one allele and has only minimal toxicity in normal peripheral blood mononucleocytes. Finally, gene expression analysis and qPCR demonstrated that the compound reduced the expression of *MYC* and MYC target genes and did not alter the expression of several other genes, capable of being controlled by G4s, thus indicating considerable selectivity.

RESULTS AND DISCUSSION

To identify compounds that selectively bind to *MYC* G4 DNA, we used a small molecule microarray (SMM) screening approach (Figure 1).[36−42] Briefly, a library of 20 000 compounds was covalently immobilized on glass slides using isocyanate surface chemistry, as previously described.[43] Next, a Cy5-labeled *MYC* G4 oligonucleotide derived from the $NHEIII_1$ region of the promoter[12] was annealed and incubated

DOI: 10.1021/acschembio.5b00577
ACS Chem. Biol. 2016, 11, 139−148

with the printed library to identify discrete binding interactions (Figure 1B). In parallel, several other Cy5-labeled oligonucleotide structures (including RNA hairpins,[43] the FOXO binding domain,[44] and CAG repeat DNA[45]), which served as controls, were screened in an analogous manner. For each compound in the library, a composite Z-score was calculated, and the *MYC* G4-incubated data set was compared to a buffer-incubated control data set. Compounds were considered hits if the composite Z-score was greater than three (representing three standard deviations from the mean of the screening library) and if no fluorescence was observed in the buffer-incubated sample. Those hit compounds found to bind other nonhomologous oligonucleotides investigated by the same technique were also eliminated from further consideration.

Using these criteria, 32 unique hit compounds were identified as binding selectively to the *MYC* G4 structure, for a final hit rate of 0.16%. We used the combination of Z-score, qualitative inspection of microarray results, and compound availability to select a panel of the 12 most promising hit compounds for further analysis (Figure S1). Each of these compounds was evaluated for its capacity to functionally inhibit *MYC* oncogene expression, and to reduce cell viability in multiple myeloma cell lines. On the basis of these preliminary studies, we identified compound **1**, a benzofuran-containing structure. In the SMM screen, **1** had a composite Z-score of 4.05 for the MYC G4 and less than 1 for CAG repeat DNA (0.10), FOXO3 DNA (0.16), HIV TAR RNA (0.45), and miR-21 RNA (−0.18). Furthermore, **1** has not been reported previously as a quadruplex-binding ligand.[19] Thus, **1** was an attractive candidate, and we continued its evaluation for further in-depth characterization (Figure 1C).

To assess the ability of compound **1** to bind to the *MYC* G4 in solution, a circular dichroism (CD)-based thermal melt experiment was employed. After annealing, the molecular ellipticity of the MYC G4 was measured by CD, where a maximum was observed at 262 nm and a minimum at 244 nm, thus confirming proper folding of the oligonucleotide into a parallel-stranded G4[46] (see Supporting Information Figure S2). To measure the melting temperature (T_m), molecular ellipticity was monitored at 262 nm as a function of temperature. Finally, a sample containing equimolar concentrations of compound **1** and the *MYC* G4 oligonucleotide was evaluated in the same experiment. Molecules that productively bind to the G4-DNA stabilize the structure, which generally increases its T_m.[47] In the presence of compound **1**, the T_m of the G4-DNA increased by 2.1 (±0.5) °C (Figures 1C and S2). Although this change in melting temperature was statistically significant, in comparison to other G4-binding molecules it is relatively modest in magnitude and an orthogonal biophysical technique was pursued to further validate binding.

To quantitatively assess the binding affinity of compound **1** with the *MYC* G4, we performed SPR experiments[48] using a biotinylated *MYC* G4 oligonucleotide. The oligonucleotide was immobilized to a streptavidin-coated chip, and binding was measured as a function of concentration (Figure 1). This experiment demonstrated that compound **1** bound to MYC G4 DNA with an equilibrium dissociation constant (K_d) of 4.5 ± 1.4 μM (Figure 1D). Importantly, **1** interacted with *MYC* G4 DNA through a reversible binding interaction as observed in the sensorgram (Figure 1D). To compare the binding of **1** to a variety of other quadruplex structures, K_d measurements were also performed by SPR on five other quadruplexes from other genes: KRAS, Bcl2, VEGF, Myb, and RB1 (Figure S3). No binding was observed up to the limit of compound solubility for KRAS, Myb, or VEGF G4s. In contrast, 3−4-fold weaker binding was measured for Bcl2 and RB1 (14 μM and 13 μM, respectively, Figure S3). In sum, the microarray screen and biophysical studies performed here demonstrate that compound **1** binds reversibly to *MYC* quadruplex DNA. Importantly, however, in the microarray analysis binding was not observed to duplex DNA structures (such as the FOXO binding domain or CAG repeat DNA) or RNA hairpins. Furthermore, while **1** binds to the MYC quadruplex, weaker or no binding is observed in five other quadruplex structures.

Next, a PCR-stop assay was used to investigate the ability of compound **1** to inhibit *MYC* DNA amplification in a G4-dependent fashion.[49,50] Under the conditions of the assay, a linear *MYC* Pu27 (mutant) sequence can be PCR-amplified using normal thermal cycling conditions. However, a G4-containing Pu27 (wild type) sequence blocks polymerase activity, thus inhibiting formation of the PCR product. In the presence of a G4-stabilizing ligand, PCR amplification is further inhibited. Indeed, compound **1** demonstrated dose-dependent inhibition of PCR amplification for the wild type Pu27 sequence at a variety of concentrations. In contrast, **1** had no effect at concentrations up to 100 μM on the amplification of a mutant sequence incapable of G4 formation and a weaker affinity of 12.7 μM to this sequence as measured by SPR (Figure 2A, Supporting Information Figure S3A). Taken together, these *in vitro* data point to a G4-dependent mechanism of inhibition by the lead compound.

To evaluate whether the effects of compound **1** on *MYC* in cells was dependent on the presence of the G4 in the promoter,

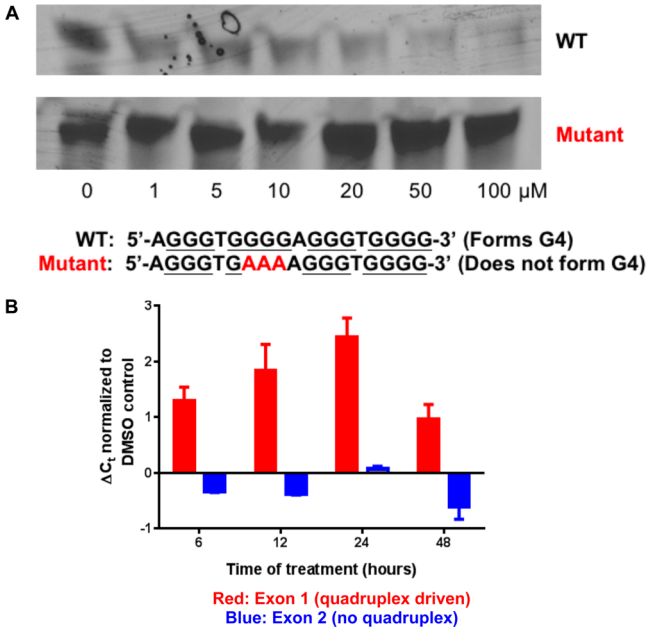

Figure 2. (A) PCR stop assay. Compound **1** inhibits PCR amplification of a synthetic wild type oligonucleotide sequence capable of forming a G4 but does not inhibit amplification of the mutant sequence that cannot form a G4. (B) Exon specific qPCR assay with the CA-46 Burkitt's lymphoma cell line. *MYC* Exon 1 (in red) remains under control of the G4, while transcription from exon 2 is not under control of a G4. Cells were treated with 10 μM **1** for the time indicated. The observed threshold cycle (Ct) by real time PCR, normalized to vehicle control, was measured. Error bars represent the standard deviation of three replicates.

DOI: 10.1021/acschembio.5b00577
ACS Chem. Biol. 2016, 11, 139−148

the CA46 Burkitt's lymphoma line was used in an exon-specific assay.[23] For most cell lines, 85−90% of MYC expression is controlled by the G4 located prior to exons 1 and 2 in the promoter. Furthermore, expression predominantly occurs following exon 2, due to a 1000-fold increase in transcription from this allele.[51] The CA46 Burkitt's lymphoma cell line is an exception due to the existence of a chromosome (8:14)[52] translocation between exons 1 and 2. In the CA46 line, only exon 1 is under G4 control, and the majority of MYC expression comes from exon 2, which is independent of G4 regulation (Figure 2B). This uncommon location for translocation insertion into the MYC locus renders the overall cell line resistant to G4-mediated MYC inhibition,[23] and proliferation should not be affected by G4-stabilizing agents. Using FAM-tagged exon specific TaqMan gene expression assays with qPCR for *MYC*, we demonstrated that treatment of CA46 with compound **1** caused down-regulation of transcription from exon 1, which contains the G4, while transcription from exon 2, which does not contain a G4, is unaffected at treatment times of up to 48 h (Figure 2B). Further, as MYC protein expression in this line is mostly due to the G4-independent translocation, MYC protein levels were unchanged in CA46 cells treated with compound **1** (Figure 3D).

Since two-thirds of multiple myeloma cases involve deregulated *MYC* expression,[53,54] we evaluated the effects of compound **1** on cell viability in 10 different multiple myeloma cell lines (Table 1). Compound **1** inhibited L363 cell viability in a dose- and time-dependent manner, with an IC_{50} of 5.8 ± 1.0 μM after 72 h. By comparison, BRACO-19, another well-studied G4-binding compound, has an IC_{50} of 15.3 μM in this cell line, which is consistent with literature values of ∼1−13 μM across several other cell lines.[33,34] Furthermore, compound **1** induced a 7-fold decrease in *MYC* transcription after 24 h of treatment in L363 cells (Figure 3A). Additionally, *MYC* protein expression was also inhibited by exposure to 10 μM of compound **1**, while vehicle treated cells showed no change in MYC protein levels (Figure 3B). MYC was also suppressed in a dose dependent manner when treated with **1** (Figure 3C). This suppression was maintained over 72 h, which is notable given the characteristic rapid replenishment of this protein[55]—a phenomenon that complicates targeting *MYC* at the protein level. Decreases in MYC protein were observed in all lines tested with **1**, and this effect also correlated with decreases in cell viability (Figure 3D). The CA46 Burkitt's lymphoma line (lacking a G4) was included in this panel as a resistant control, and it showed negligible changes in *MYC* expression or cell viability when treated with compound **1**. In addition, at a concentration of 10 μM, compound **1** did not alter viability of peripheral blood mononucleocytes drawn from a healthy volunteer (Figure 3D).

To further explore the mechanism of action of compound **1** on myeloma cells, we performed cell cycle analysis and monitored the cells for apoptosis. Compound **1** caused ∼85% of the treated cells to arrest in the G1 phase after 72 h, as measured by flow cytometric analysis of propidium iodide stained cells (Figure 4A), and increased apoptosis from 7% in untreated cells to 13% of treated cells, as measured by Annexin V/7-AAD staining (Figure 4B). The minimal induction of apoptosis observed by Annexin V staining was supported by Western blots for activation (proteolytic cleavage) of the apoptotic mediator, caspase 3 (Supporting Information Figure S4). Additionally, the compound triggered a substantial increase in senescence-associated β-galactocidase staining in

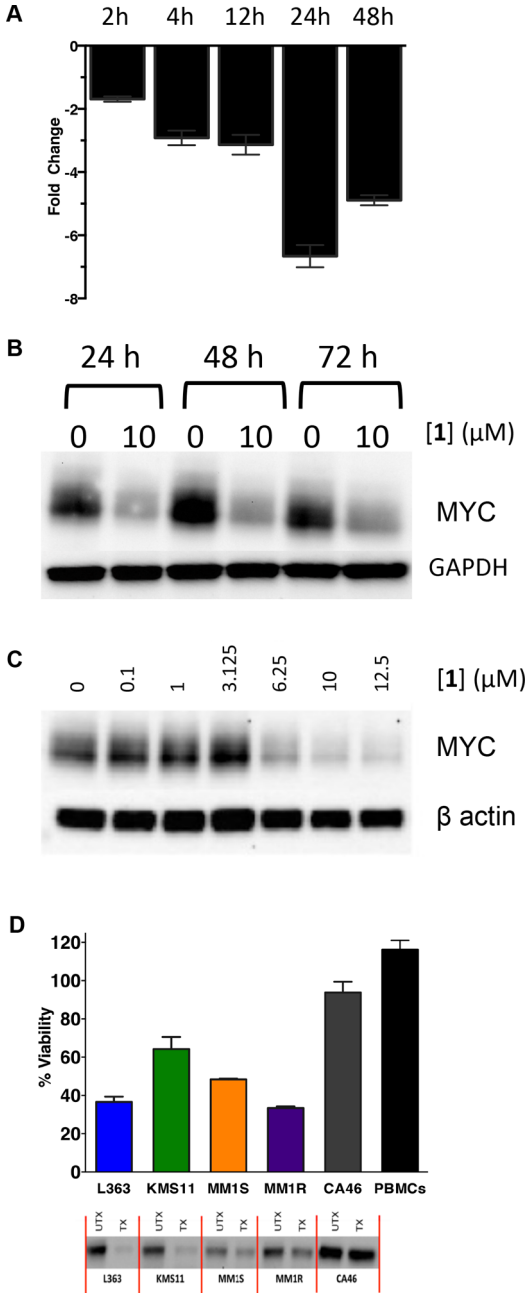

Figure 3. (A) Time-dependent inhibition of *MYC* transcription in myeloma cells after treatment with 10 μM **1**, as measured by qPCR. Fold change is measured by the difference with respect to the untreated vehicle. Data are the average of two replicates, ± SEM. (B) Inhibition of MYC protein translation with 10 μM compound **1** is sustained over time. (C) MYC protein levels are inhibited as a function of the dose of **1**. (D) Effects on cell viability and MYC protein translation by compound **1** across a panel of multiple myeloma cell lines. Also included are the resistant CA46 Burkitt's lymphoma cell line and peripheral blood mononucleocytes. Data are the average of three replicates, ± SEM (n = 4).

myeloma cells after 72 h of treatment, supporting cell cycle arrest/senescence as a primary mechanism of action (Figure 4C). Taken together, these results support the conclusion that compound **1** is acting through suppression of MYC expression, rather than a nonspecific mechanism of action.

To further explore the specificity of compound **1**, we evaluated its effects on the expression of a panel of 770 cancer-

DOI: 10.1021/acschembio.5b00577
ACS Chem. Biol. 2016, 11, 139−148

Table 1. Cytotoxicity Measurements for 1 against Multiple Myeloma Cell Lines (72 h Treatment)[a]

compound	cell line	IC_{50} (μM)
1	L363	5.8 ± 1.0
1	KMS12PE	6.5 ± 0.7
1	MOLP8	8.3 ± 2.9
1	LP1	8.3 ± 1.0
1	KMS27	9.6 ± 1.0
1	AMO1	11.3 ± 0.9
1	ARD	12.9 ± 1.4
1	JIM1	14.1 ± 1.3
1	KMM1	15.6 ± 4.4
1	8226	15.9 ± 2.3
BRACO-19	L363	15.3 ± 4.3

[a]Values represent the average of four replicates ± SEM.

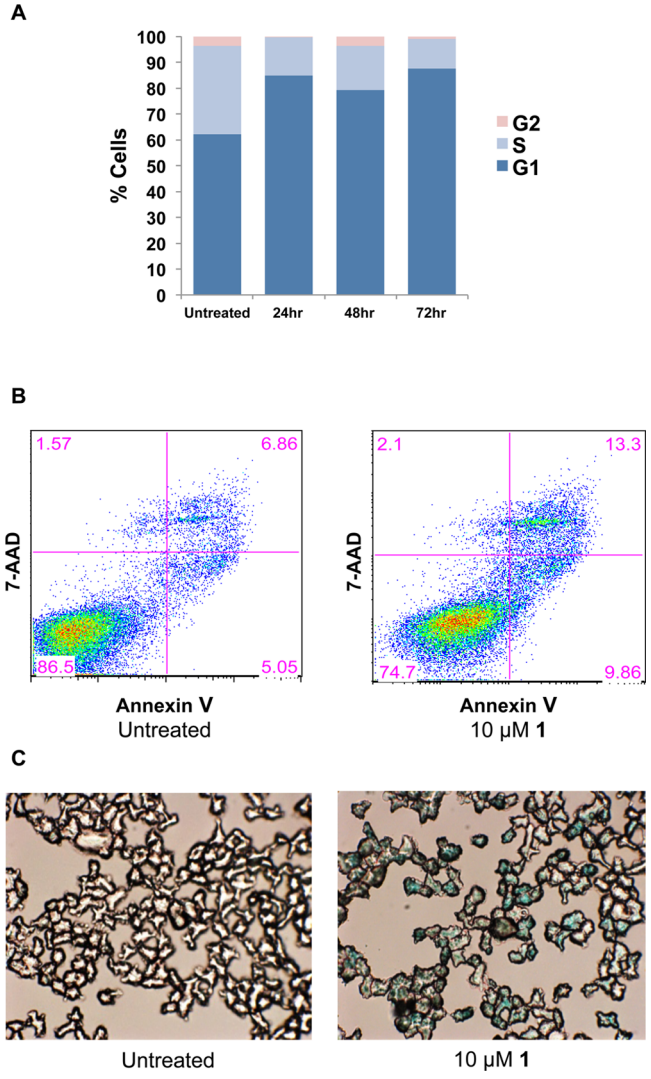

Figure 4. (A) Cell cycle analysis for L363 cells treated with 10 μM **1**. Compound **1** induces sustained G1 arrest. (B) Compound **1** does not induce significant apoptosis at 10 μM after 72 h, as seen by the difference between untreated (left panel) and treated (right panel) cells. (C) Compound **1** induces a senescent state in myeloma cells at 10 μM after 72 h (senescent cells are stained blue).

associated genes in a quantitative, digital gene expression assay (Nanostring) in L363 cells.[56] In addition to *MYC* itself, several MYC target genes were included in the panel, as were a number of other G4-driven genes. Cells were treated with 10 μM of compound **1** for 2, 4, 12, 24, and 48 h and separately at concentrations of 1, 2.5, 5, and 10 μM for 24h, and the effects on gene expression were evaluated. In Figure 5A, the 145 genes whose expression changed ≥1.5 fold in at least one of the five time or dose points are reported. In the heatmaps, Log2 fold changes relative to a vehicle (DMSO) treated control are shown (Figure 5A). Gene expression was modulated as a function of both time and concentration of **1**. Importantly, *MYC* was one of the most suppressed genes. Furthermore, after 4 h, a number of known MYC target genes were also suppressed, including E2F1, MCM2, MCM4, MCM5, and CDC25A. Expression levels of the known MYC target gene E2F1 were also validated in additional experiments by qPCR (Supporting Information Figure S5). A third data set was collected to compare compound **1** to JQ-1 (a BET-bromodomain inhibitor) and quarfloxin (another G4-binding small molecule; Figure 5A). All three inhibitors exhibited substantial nonoverlapping differences in their gene expression profiles, highlighting the distinct mechanism of action of compound **1**.

As evaluating specificity was a principal goal of this experiment, the effects of compound **1** on a number of known G4-driven genes in the panel were examined further. Expression levels of *MYC*, *RB1*, *VEGFA*, *KRAS*, and *HIF1α*, all of which are reported to be under the control of promoter G4s, and are expressed in L363 cells, were included in the panel of genes evaluated in Figure 5A. The change in expression for each of these genes (nanostring) over time is presented in Figure 5B. While *MYC* expression was substantially reduced at all time points, expression of other G4-associated genes was minimally affected. To further confirm these results, we also performed qPCR experiments on the same five genes (Figure 5C). Again, MYC expression is greatly reduced while other genes are minimally affected. These changes in gene expression are in line with biophysical measurements of compound affinity. While the quadruplex with the highest affinity for **1** (MYC) had pronounced changes in gene expression, G4s with weaker binding (RB1, BCL2) or a complete lack of G4 binding (KRAS, VEGF) had minimal changes in expression, even after 48 h of treatment.

Having established the reversible binding of compound **1** to the MYC G4 DNA and its G4-dependent silencing of MYC, a remaining consideration was the presence of a benzylamino-phenol functional group in compound **1**. It has previously been reported that compounds containing this functional group can have the propensity to eject amines, form an *o*-quinone methide, and alkylate proteins or DNA.[57−59] To assess whether compound **1** was undergoing this reactivity, a small series of analogs was prepared (Figure S6). In Figure 5D, compounds lacking the phenol or amino group were prepared and evaluated. Compound **2** (lacking the amino substitution) was not active, while compound **3** (incapable of forming a quinone methide) retained some activity in silencing *MYC* expression, demonstrating the importance of the amino group for activity. Further evidence supporting the role of these functional groups in binding is evidenced in SPR experiments (Figure S7), where compound **2** did not bind to the G4 and compound **3** bound, but with weaker affinity than **1**. The stability of compound **1** was also evaluated by LC/MS (see Supporting Information, Figure S8). Here, it persisted in culture media over a period of 72 h, confirming that the compound is largely stable in

DOI: 10.1021/acschembio.5b00577
ACS Chem. Biol. 2016, 11, 139−148

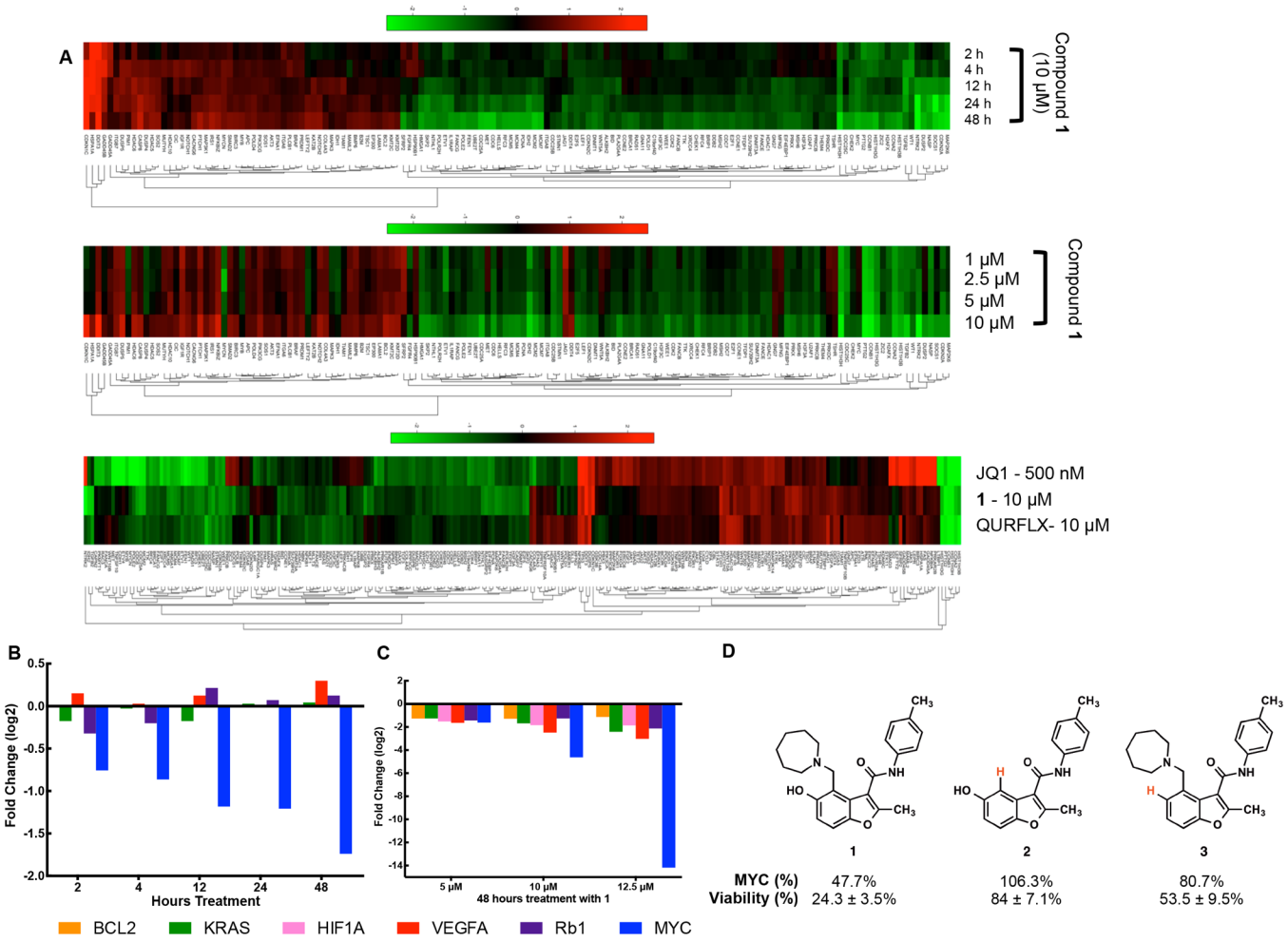

Figure 5. Gene expression data. (A) Effects of compound **1** on expression of genes (Nanostring) at various time points (at 10 μM), doses (1−10 μM), and in comparison to both JQ1 (500 nM) and Quarfloxin (10 μM). (B) Effects of **1** on a panel of known G4-controlled genes. Data are presented from the experiments described in A at 10 μM treatment for several time points (Log2 fold change). (C) qPCR analysis of G4-associated genes at 48 h treatment with 10 μM **1** (data are the average log2 value for $\Delta\Delta C_t$ of three replicates). (D) Structures and effects on MYC protein expression and cell viability in L363 myeloma cells treated with compound **1** and two analogs lacking key functional groups. Cells were treated with 10 μM of each compound for 24 h. Values represent the mean of three experiments ± standard deviation.

complex, biologically relevant mixtures over the time frame of viability and gene expression assays used in this study. Additionally, the putative hydrolysis product arising from quinone methide formation was not observed at any time by LC/MS, further suggesting that compound **1** is unlikely to have a high propensity to form a quinone methide.

CONCLUSION

In conclusion, we have utilized a SMM screening approach to identify a new small molecule G4 stabilizing compound that transcriptionally silences *MYC* expression in myeloma cells. The development of such molecules is an attractive alternative to the direct inhibition of MYC protein activity. By evaluating multiple oligonucleotide structures simultaneously as part of the initial screen, selectivity considerations were incorporated early in the discovery process. Binding affinity, coupled with decreases in MYC protein expression and cell viability, led to the identification of a novel G4-binding benzofuran scaffold, compound **1**, that specifically inhibited G4-dependent *MYC* expression in myeloma cells. This relatively stable compound binds reversibly to the *MYC* G4 with an equilibrium dissociation constant of 4.5 μM. Further, weaker or no binding was observed in a variety of other G4 structures in SPR experiments. While MYC is silenced in cellular models, other G4-driven genes are silenced transiently or not at all. Differential binding to quadruplexes may be considered as a mechanism for the observed biological selectivity. An analog of **1** lacking the amine was completely inactive, while an analog lacking the phenol group (incapable of forming a quinone methide) retained some activity. Thus, the amine functionality may be required for binding to the quadruplex, while the formation of a quinone methide structure may not be. G1 arrest and senescence were triggered in myeloma cell lines, whereas the viability of normal human mononucleocytes was only modestly affected. Transcriptional profiling of genes affected by **1** revealed it induced a decrease in the expression of *MYC* and MYC target genes as a function of both time and dose. Furthermore, **1** displayed a gene expression profile distinct from that produced by JQ1, a BET bromodomain inhibitor known to decrease *MYC* expression, and quarfloxin, another G4-binding compound. This unique and selective expression profile is particularly notable given the role of MYC in controlling the expression of a large number of genes within the genome, and its relevance to cancer. Combined with the lack of

DOI: 10.1021/acschembio.5b00577
ACS Chem. Biol. 2016, 11, 139−148

toxicity to cells where MYC is not under the control of a G4, or to PBMCs, the selective toxicity and MYC silencing activity exhibited by **1** make it an attractive candidate for further study.

Although modulation of oncogene expression via G4 stabilization holds much promise as a therapeutic approach, there is not yet a clinically approved G4 stabilizing drug. Thus, the discovery and study of new chemical scaffolds that modulate quadruplex-driven gene expression, and technologies that enable such discoveries, remain areas of high importance. The selective modulation of MYC protein expression levels itself is also a highly desirable goal from a therapeutic standpoint, where chemical inhibition of MYC has been long sought after and is generally difficult to achieve. We hypothesize that compound **1**, or a more potent derivative, would have high utility in this regard. Furthermore, given the emergence of numerous G4s as regulatory elements in a variety of genes,[60] the SMM approach may be broadly applicable to rapidly identifying new classes of selective G4-stabilizing small molecule scaffolds for other genes as well.

MATERIALS AND METHODS

Small Molecule Microarray Screening. Small molecule microarray screening was carried out as previously described.[37,43,61] Briefly, γ-aminopropyl silane (GAPS) microscope slides were functionalized with a short Fmoc-protected amino polyethylene glycol spacer. After deprotection using piperidine, 1,6-diisocyanatohexane was coupled to the surface by urea bond formation to provide functionalized isocyanate-coated microarray slides that can react with primary alcohols and amines to form immobilized chemical screening libraries. A total of 20 000 unique small molecule stock solutions (10 mM in DMSO) purchased from ChemBridge and ChemDiv screening libraries, in addition to dyes and controls, were printed in duplicate onto four slides of 5000 compounds each and exposed to pyridine vapor to facilitate covalent attachment to the slide surface. After drying, slides were incubated with a polyethylene glycol solution to quench unreacted isocyanate surface. Printed slides were incubated for 1 h at RT with a Cy5-tagged DNA oligonucleotide of the *MYC* G4 forming sequence (5′d(Cy5)-TGAGGGTGGGTAGGGTGGGTAA-3′), which had been annealed by heating to 95 °C for 3 min, cooled to RT, and diluted to 500 nM in PBS. Following incubation, slides were gently washed three times for 5 min in PBST, twice in PBS, and once in deionized water to remove unbound oligonucleotide and dried by centrifugation for 2 min at 3400*g*. Fluorescence intensity was measured (650 nm excitation, 670 nm emission) on a GenePix 4000a Microarray Scanner. Hits were identified on the basis of signal-to-noise ratio (SNR), defined as mean foreground − mean background/standard deviation of background, and Z-score, with the following criteria: (1) Raw SNR > 0, (2) SNR > 3 SD above negative control readings, (3) coefficient of variance (CV) of replicate spots <100, (4) SNR of negative control slide <1, and (5) no activity with any other nucleic acid structures screened. The other nucleic acids were the FOXO3 DNA transcription factor binding domain, CAG DNA repeat, HIV TAR RNA, and miR-21 RNA, all of which were Cy5-labeled, and the screens were run in the same method described above using the respective Cy5-nucleic acid instead of the *MYC* DNA.

PCR Stop Assay. A test oligonucleotide and a complementary sequence that partially hybridizes to its last repeat (sequences below) were synthesized by IDT. The reactions were performed in a master mix containing 1× PCR buffer, 10 μmol of each oligo, 0.16 mM dNTP, 1.5 mM $MgCl_2$, 2.5 U HotStarTaq polymerase (Qiagen), and a dose titration of a ligand of interest, spanning 3 orders of magnitude, in 25 μL total volume. The thermal cycling conditions were as follows: 94 °C for 5 min, followed by 22 cycles of 94 °C for 30 s, 58 °C for 30 s, 72 °C for 30 s, and finally held at 4 °C following completion. The amplified products were mixed with 6× DNA loading dye (Thermo Scientific) and resolved on a 15% TBE-Urea Gel (Invitrogen) on the Novex mini gel system at 150 V for 1 h. The gel products were stained in a 0.01% (v/v) ethidium bromide-TBE solution for 15 min and imaged under UV light on the GBOX F3 (Syngene).

Oligos used. Forward: 5′-AGG GTG GGG AGG GTG GGG-3′ (partial sequence in the promoter of oncogene *MYC* that may form G4)

Forward mutant: 5′-AGG GTG AAA AGG GTG GGG-3′

Reverse: 5′-ATC GAT CGC TTC TCG TCC TTC CCC A-3′ (complementary sequence used for both forward and reverse)

Exon Specific Assay. CA46 cells were treated with ligands of interest or DMSO control at designated time points, washed in PBS, flash frozen, and RNA isolated using the Qiagen RNeasy Kit. RNA was quantified by NanoDrop, and 0.5 μg was reverse transcribed for use in qPCR. Reverse transcription was performed using the Applied Biosystems Kit B808−0234, cycled at 25 °C for 10 min, 48 °C for 60 min, 95 °C for 5 min, and held at 4 °C following completion in 25 μL total volumes. The cDNA was diluted 4-fold and used in qPCR with the Taqman Gene Expression Assays (Life Technologies, exon 1:01562521_m1, exon 2:00153408_m1), cycled at 50 °C for 2 min, 95 °C for 10 min, and followed by 40 cycles of 95 °C for 15 s and 60 °C for 1 min on the Applied Biosystems 7500 Fast Real-Time PCR System. For exon 1 and exon 2, ΔC_t was normalized to a VIC-Primer Limited tagged GAPDH Taqman Gene Expression Assay (multiplexed in the same well) and DMSO treated control samples.

Thermal Melt Assay. Thermal stability of the *MYC* G4-forming oligonucleotide Pu22 (**TGAGGGTGGGTAGGGTGGGTAA**) in the absence and presence of compounds was recorded on an Aviv Biomedical Inc. Model 420 Circular Dichroism Spectrometer. The *MYC* G4 was diluted to 50 μM in 10 mM Tris buffer (pH 7.5, containing 100 mM KCl), heated to 95 °C for 5 min, and allowed to cool to RT. Positive molecular ellipticity of the parallel G4 peak (262 nm) was confirmed by spectral examination. To 150 μL of the G4 in buffer was added 1 equiv of compound (150 μL of a 50 μM solution in buffer containing 0.5% DMSO), after which the mixtures were heated from 5 to 95 °C at 2 °C/min in a 0.1 mm quartz cell. Molecular ellipticity as a function of temperature was used to calculate a T_m (the temperature at which 50% of the formed higher order DNA structure was melted) for each condition using GraphPad Prism 6 software and a nonlinear regression model with a variable slope. ΔT_m values were calculated as $T_{m(+compound)} - T_{m(control)}$.

Surface Plasmon Resonance (SPR). SPR experiments were performed with a Biacore T200 (GE Healthcare). A total of 20 μg/mL biotin-labeled Pu22 G4 in 10 mM Tris buffer (pH 7.5, containing 100 mM KCl, 3 mM EDTA) was heated to 95 °C for 5 min, and allowed to cool to RT. The *MYC* DNA was then captured (FC2:1245 Ru) on a Series S Sensor CM5 Chip (GE Healthcare) with amine-coupled Neutravidin (FC1:4466 Ru, FC2:5458 Ru). Single cycle kinetics (SCK) experiments were carried out with five injections of increasing concentration of analyte solution, which was prepared by a 3-fold serial dilution of compound with buffer (10 mM Tris pH 7.5, 100 mM KCl, 3 mM EDTA) containing 3% DMSO. Binding analysis was conducted at a flow rate of 30 μL/min at 25 °C. In each run, the association phase and the subsequent dissociation phase were monitored for 1 and 10 min, respectively. Prior to each compound injection, three buffer injections were made. From the obtained reference-subtracted sensorgrams, the dissociation constants (K_d) of the compounds were estimated by a global fitting to a simple 1:1 binding model in the Biacore evaluation software (GE Healthcare).

Cell Culture Conditions and Experimental End points. Human multiple myeloma and Burkitt's lymphoma cell lines L363, CA46, MM-1R, KMS-11, MM-1S, 8226, ARD, JIM1, KMM1, LP1, KMS27, AMO1, KMS12PE, and MOLP8 were cultured and authenticated as previously described.[62] All cell lines were cultured in RPMI-1640 (2 mM L-glutamine, 10% fetal bovine serum (FBS), 100 U/mL penicillin, 100 μg/mL streptomycin: Gibco) and incubated at 37 °C with 5% CO_2. Viability experiments were performed in quadruplicate on 96-well plates (Costar) at designated time and dose points. The MTS reagent was then directly added and incubated at 37 °C for 90 min, and the absorbance of MTS formazan was read at 500 nm on an Omega 640 spectrophotometer. Percentage cell viability was normalized to the absorbance of untreated (DMSO) wells.

DOI: 10.1021/acschembio.5b00577
ACS Chem. Biol. 2016, 11, 139−148

In the case of cells harvested for their protein or RNA, pellets were flash frozen and stored at −80 °C overnight prior to use. For cell cycle analyses, 2×10^6 cells were washed with cold PBS and fixed with 1 mL of 70% ethanol for 30 min. Cells were stained with 0.5 mL PI/Rnase staining buffer (BD, Catalog #: 550825) for 15 min at RT and analyzed by flow cytometry (BD FACSCalibur). Data were analyzed and generated by Modfit LT. For apoptosis assays, 2×10^6 cells were washed twice with cold PBS and cells were stained following the protocol from the PE Annexin V Apoptosis Detection Kit I (BD, Catalog #: 559763). The stained cells were analyzed by flow cytometry (BD FACSCalibur) within 1 h. Data were analyzed with FlowJo.

β-Galactosidase staining to detect senescent cells was performed using Senescence β-Galactoside Staining Kit (Cell Signaling Technology #9860). L363 cells treated with and without 10 μM of compound **1** were stained with the chromogenic substrate X-gal overnight in a dry incubator without CO_2. Standard experimental procedure was followed per manufacturer's protocol at pH 6. β-Galactosidase activity is present in senescent cells but not quiescent or immortalized cells at pH 6.

Western Blots. Cell pellets were homogenized and lysed in RIPA buffer on ice for 1 h. Protein was quantitated by BCA, and equal protein was loaded onto 4−12% Bis-Tris Gels (Novex), electrophoresed at 150 V for 75 min to obtain sufficient separation, and transferred with the iBlot system (Life Technologies). Successful transfer and uniform loading was confirmed by Ponceau S staining (Thermo Scientific). Blots were blocked in 10% dry milk in TBST, incubated with primary monoclonal antibodies in 5% BSA at concentrations designated by the manufacturer, and gently rotated at 4 °C overnight. Blots were washed with TBST three times prior to incubation with polyclonal secondary antibodies for 1 h in 5% dry milk at RT. Blots were washed three more times with TBST and imaged with Supersignal West Dura Chemiluminescent Substrate (Thermo Scientific) on the GBOX F3 (Syngene). The MYC monoclonal antibody was purchased from Abcam (ab84132) and used at a concentration of 1:1000. All other monoclonal antibodies were purchased from Cell Signaling Technologies and used at a concentration of 1:1000, with the exception of α−β tubulin, which was used at a concentration of 1:2000. All primary antibodies used in this study were of rabbit origin, and goat antirabbit IgG (H+L) horseradish peroxidase conjugate (Invitrogen G21234) was used as the polyclonal secondary antibody at a concentration of 1:4000. For better quantitation of MYC protein, a size based automated capillary immunoassay system (Simple Western, ProteinSimple, Santa Clara, CA) was performed by the Center for Cancer Research Collaborative Protein Technology Resource Group according to manufacturer's protocols.[63]

Cancer Genome-Wide Probing and Statistical Packaging. Myeloma cells were treated with 10 μM of compound **1**, 500 nM JQ1, and 10 μM of Quarfloxin for 24 h. RNA of treated myeloma cells at designated time points (2, 4, 12, 24, 48 h) and doses (1, 2.5, 5, and 10 μM) was isolated with the Qiagen RNeasy kit and used with the nCounter Human Cancer Reference Kit (NanoString Technologies), surveying changes in expression for 780 cancer-related human genes and six reference genes. Quantitative changes in expression were analyzed and grouped in the form of a heat map using the programming language R. All other quantitative statistical analyses were performed in GraphPad Prism.

■ ASSOCIATED CONTENT

Supporting Information

The Supporting Information is available free of charge on the ACS Publications website at DOI: 10.1021/acschembio.5b00577.

SMM hit structures, CD spectrum of the MYC G4 DNA, SPR sensorgrams and K_d measurements, caspase and PARP cleavage assays, qPCR data, synthetic procedures and characterization data, and stability study for compound **1** (PDF)

Data for time, dose, and other compounds (XLSX)

■ AUTHOR INFORMATION

Corresponding Authors

*E-mail: mockb@mail.nih.gov.

*E-mail: schneeklothjs@mail.nih.gov.

Present Address

⊥University of Colorado Medical Scientist Training Program, Aurora, CO

Author Contributions

#These authors contributed equally.

Notes

The authors declare no competing financial interest.

■ ACKNOWLEDGMENTS

We thank members of the Chemical Biology Laboratory for helpful comments and suggestions. We gratefully acknowledge Dr. A. Stephen, K. Worthy, Dr. M. O'Neill, Dr. T. Anderson, and the Protein Chemistry Laboratory (Advanced Technology Program, Frederick National Laboratory for Cancer Research) for their invaluable expertise and assistance in conducting the surface plasmon resonance experiments. We thank J.-Q. Chen and M. A. Herrmann for performing the MYC immunoassays with Protein Simple technology. We thank G. Tosato (Center for Cancer Research) for the CA46 cells. We also thank J. Merkel for helpful discussions regarding microarray analysis. This work was supported by the Intramural Research Program of the National Institutes of Health, Center for Cancer Research, and the National Cancer Institute (NCI), National Institutes of Health (1 ZIA BC011585 01). K.F. obtained his M.S., and E.L. is working on her M.S. as NCI/Johns Hopkins University Molecular Targets and Drug Discovery Fellows. J.K.S. is a Multiple Myeloma Research Foundation fellow.

■ REFERENCES

(1) Bretones, G., Delgado, M. D., and Leon, J. (2014) Myc and cell cycle control. *Biochim. Biophys. Acta, Gene Regul. Mech. 1849*, 506−516.

(2) Beroukhim, R., Mermel, C. H., Porter, D., Wei, G., Raychaudhuri, S., Donovan, J., Barretina, J., Boehm, J. S., Dobson, J., Urashima, M., Mc Henry, K. T., Pinchback, R. M., Ligon, A. H., Cho, Y. J., Haery, L., Greulich, H., Reich, M., Winckler, W., Lawrence, M. S., Weir, B. A., Tanaka, K. E., Chiang, D. Y., Bass, A. J., Loo, A., Hoffman, C., Prensner, J., Liefeld, T., Gao, Q., Yecies, D., Signoretti, S., Maher, E., Kaye, F. J., Sasaki, H., Tepper, J. E., Fletcher, J. A., Tabernero, J., Baselga, J., Tsao, M. S., Demichelis, F., Rubin, M. A., Janne, P. A., Daly, M. J., Nucera, C., Levine, R. L., Ebert, B. L., Gabriel, S., Rustgi, A. K., Antonescu, C. R., Ladanyi, M., Letai, A., Garraway, L. A., Loda, M., Beer, D. G., True, L. D., Okamoto, A., Pomeroy, S. L., Singer, S., Golub, T. R., Lander, E. S., Getz, G., Sellers, W. R., and Meyerson, M. (2010) The landscape of somatic copy-number alteration across human cancers. *Nature 463*, 899−905.

(3) Berg, T., Cohen, S. B., Desharnais, J., Sonderegger, C., Maslyar, D. J., Goldberg, J., Boger, D. L., and Vogt, P. K. (2002) Small-molecule antagonists of Myc/Max dimerization inhibit Myc-induced transformation of chicken embryo fibroblasts. *Proc. Natl. Acad. Sci. U. S. A. 99*, 3830−3835.

(4) Yin, X., Giap, C., Lazo, J. S., and Prochownik, E. V. (2003) Low molecular weight inhibitors of Myc-Max interaction and function. *Oncogene 22*, 6151−6159.

(5) Huang, M. J., Cheng, Y. C., Liu, C. R., Lin, S., and Liu, H. E. (2006) A small-molecule c-Myc inhibitor, 10058-F4, induces cell-cycle arrest, apoptosis, and myeloid differentiation of human acute myeloid leukemia. *Exp. Hematol. 34*, 1480−1489.

DOI: 10.1021/acschembio.5b00577
ACS Chem. Biol. 2016, 11, 139−148

(6) Wang, H., Hammoudeh, D. I., Follis, A. V., Reese, B. E., Lazo, J. S., Metallo, S. J., and Prochownik, E. V. (2007) Improved low molecular weight Myc-Max inhibitors. *Mol. Cancer Ther. 6*, 2399−2408.
(7) Delmore, J. E., Issa, G. C., Lemieux, M. E., Rahl, P. B., Shi, J., Jacobs, H. M., Kastritis, E., Gilpatrick, T., Paranal, R. M., Qi, J., Chesi, M., Schinzel, A. C., McKeown, M. R., Heffernan, T. P., Vakoc, C. R., Bergsagel, P. L., Ghobrial, I. M., Richardson, P. G., Young, R. A., Hahn, W. C., Anderson, K. C., Kung, A. L., Bradner, J. E., and Mitsiades, C. S. (2011) BET bromodomain inhibition as a therapeutic strategy to target c-Myc. *Cell 146*, 904−917.
(8) Dang, C. V., O'Donnell, K. A., Zeller, K. I., Nguyen, T., Osthus, R. C., and Li, F. (2006) The c-Myc target gene network. *Semin. Cancer Biol. 16*, 253−264.
(9) Balasubramanian, S., Hurley, L. H., and Neidle, S. (2011) Targeting G-quadruplexes in gene promoters: a novel anticancer strategy? *Nat. Rev. Drug Discovery 10*, 261−275.
(10) Huppert, J. L., and Balasubramanian, S. (2007) G-quadruplexes in promoters throughout the human genome. *Nucleic Acids Res. 35*, 406−413.
(11) Gray, L. T., Vallur, A. C., Eddy, J., and Maizels, N. (2014) G quadruplexes are genomewide targets of transcriptional helicases XPB and XPD. *Nat. Chem. Biol. 10*, 313−318.
(12) Gonzalez, V., and Hurley, L. H. (2010) The c-MYC NHE III(1): function and regulation. *Annu. Rev. Pharmacol. Toxicol. 50*, 111−129.
(13) Weitzmann, M. N., Woodford, K. J., and Usdin, K. (1996) The development and use of a DNA polymerase arrest assay for the evaluation of parameters affecting intrastrand tetraplex formation. *J. Biol. Chem. 271*, 20958−20964.
(14) Brooks, T. A., and Hurley, L. H. (2010) Targeting MYC Expression through G-Quadruplexes. *Genes Cancer 1*, 641−649.
(15) Kang, H. J., Le, T. V., Kim, K., Hur, J., Kim, K. K., and Park, H. J. (2014) Novel interaction of the Z-DNA binding domain of human ADAR1 with the oncogenic c-Myc promoter G-quadruplex. *J. Mol. Biol. 426*, 2594−2604.
(16) Siddiqui-Jain, A., Grand, C. L., Bearss, D. J., and Hurley, L. H. (2002) Direct evidence for a G-quadruplex in a promoter region and its targeting with a small molecule to repress c-MYC transcription. *Proc. Natl. Acad. Sci. U. S. A. 99*, 11593−11598.
(17) Chen, B. J., Wu, Y. L., Tanaka, Y., and Zhang, W. (2014) Small Molecules Targeting c-Myc Oncogene: Promising Anti-Cancer Therapeutics. *Int. J. Biol. Sci. 10*, 1084−1096.
(18) Dash, J., Waller, Z. A., Pantos, G. D., and Balasubramanian, S. (2011) Synthesis and binding studies of novel diethynyl-pyridine amides with genomic promoter DNA G-quadruplexes. *Chem. - Eur. J. 17*, 4571−4581.
(19) Vy Thi Le, T., Han, S., Chae, J., and Park, H. J. (2012) G-quadruplex binding ligands: from naturally occurring to rationally designed molecules. *Curr. Pharm. Des. 18*, 1948−1972.
(20) Castillo-Gonzalez, D., Perez-Machado, G., Guedin, A., Mergny, J. L., and Cabrera-Perez, M. A. (2013) FDA-approved drugs selected using virtual screening bind specifically to G-quadruplex DNA. *Curr. Pharm. Des. 19*, 2164−2173.
(21) Wei, C., Ren, L., and Gao, N. (2013) Interactions of terpyridines and their Pt(II) complexes with G-quadruplex DNAs and telomerase inhibition. *Int. J. Biol. Macromol. 57*, 1−8.
(22) Nasiri, H. R., Bell, N. M., McLuckie, K. I., Husby, J., Abell, C., Neidle, S., and Balasubramanian, S. (2014) Targeting a c-MYC G-quadruplex DNA with a fragment library. *Chem. Commun. (Cambridge, U. K.) 50*, 1704−1707.
(23) Boddupally, P. V., Hahn, S., Beman, C., De, B., Brooks, T. A., Gokhale, V., and Hurley, L. H. (2012) Anticancer activity and cellular repression of c-MYC by the G-quadruplex-stabilizing 11-piperazinyl-quindoline is not dependent on direct targeting of the G-quadruplex in the c-MYC promoter. *J. Med. Chem. 55*, 6076−6086.
(24) Drygin, D., Siddiqui-Jain, A., O'Brien, S., Schwaebe, M., Lin, A., Bliesath, J., Ho, C. B., Proffitt, C., Trent, K., Whitten, J. P., Lim, J. K., Von Hoff, D., Anderes, K., and Rice, W. G. (2009) Anticancer activity of CX-3543: a direct inhibitor of rRNA biogenesis. *Cancer Res. 69*, 7653−7661.
(25) Dai, J., Carver, M., Hurley, L. H., and Yang, D. (2011) Solution structure of a 2:1 quindoline-c-MYC G-quadruplex: insights into G-quadruplex-interactive small molecule drug design. *J. Am. Chem. Soc. 133*, 17673−17680.
(26) Ohnmacht, S. A., and Neidle, S. (2014) Small-molecule quadruplex-targeted drug discovery. *Bioorg. Med. Chem. Lett. 24*, 2602−2612.
(27) Freyer, M. W., Buscaglia, R., Kaplan, K., Cashman, D., Hurley, L. H., and Lewis, E. A. (2007) Biophysical studies of the c-MYC NHE III1 promoter: model quadruplex interactions with a cationic porphyrin. *Biophys. J. 92*, 2007−2015.
(28) Sibata, C. H., Colussi, V. C., Oleinick, N. L., and Kinsella, T. J. (2001) Photodynamic therapy in oncology. *Expert Opin. Pharmacother. 2*, 917−927.
(29) Grand, C. L., Han, H., Munoz, R. M., Weitman, S., Von Hoff, D. D., Hurley, L. H., and Bearss, D. J. (2002) The cationic porphyrin TMPyP4 down-regulates c-MYC and human telomerase reverse transcriptase expression and inhibits tumor growth in vivo. *Mol. Cancer Ther. 1*, 565−573.
(30) Mikami-Terao, Y., Akiyama, M., Yuza, Y., Yanagisawa, T., Yamada, O., and Yamada, H. (2008) Antitumor activity of G-quadruplex-interactive agent TMPyP4 in K562 leukemic cells. *Cancer Lett. 261*, 226−234.
(31) Koirala, D., Dhakal, S., Ashbridge, B., Sannohe, Y., Rodriguez, R., Sugiyama, H., Balasubramanian, S., and Mao, H. (2011) A single-molecule platform for investigation of interactions between G-quadruplexes and small-molecule ligands. *Nat. Chem. 3*, 782−787.
(32) Muller, S., Sanders, D. A., Di Antonio, M., Matsis, S., Riou, J. F., Rodriguez, R., and Balasubramanian, S. (2012) Pyridostatin analogues promote telomere dysfunction and long-term growth inhibition in human cancer cells. *Org. Biomol. Chem. 10*, 6537−6546.
(33) Read, M., Harrison, R. J., Romagnoli, B., Tanious, F. A., Gowan, S. H., Reszka, A. P., Wilson, W. D., Kelland, L. R., and Neidle, S. (2001) Structure-based design of selective and potent G quadruplex-mediated telomerase inhibitors. *Proc. Natl. Acad. Sci. U. S. A. 98*, 4844−4849.
(34) Burger, A. M., Dai, F. P., Schultes, C. M., Reszka, A. P., Moore, M. J., Double, J. A., and Neidle, S. (2005) The G-quadruplex-interactive molecule BRACO-19 inhibits tumor growth, consistent with telomere targeting and interference with telomerase function. *Cancer Res. 65*, 1489−1496.
(35) Martins, C., Gunaratnam, M., Stuart, J., Makwana, V., Greciano, O., Reszka, A. P., Kelland, L. R., and Neidle, S. (2007) Structure-based design of benzylamino-acridine compounds as G-quadruplex DNA telomere targeting agents. *Bioorg. Med. Chem. Lett. 17*, 2293−2298.
(36) Bradner, J. E., McPherson, O. M., and Koehler, A. N. (2006) A method for the covalent capture and screening of diverse small molecules in a microarray format. *Nat. Protoc 1*, 2344−2352.
(37) Duffner, J. L., Clemons, P. A., and Koehler, A. N. (2007) A pipeline for ligand discovery using small-molecule microarrays. *Curr. Opin. Chem. Biol. 11*, 74−82.
(38) Kawasumi, M., Bradner, J., Kim, Y., Koehler, A., Mazitschek, R., Schreiber, S., and Nghiem, P. (2005) Small molecule microarrays to discover compounds that modulate cell cycle checkpoint function. *J. Invest. Dermatol. 124*, A39−A39.
(39) Koehler, A. N., Shamji, A. F., and Schreiber, S. L. (2003) Discovery of an inhibitor of a transcription factor using small molecule microarrays and diversity-oriented synthesis. *J. Am. Chem. Soc. 125*, 8420−8421.
(40) Miao, H., Tallarico, J. A., Hayakawa, H., Munger, K., Duffner, J. L., Koehler, A. N., Schreiber, S. L., and Lewis, T. A. (2007) Ring-opening and ring-closing reactions of a shikimic acid-derived substrate leading to diverse small molecules. *J. Comb. Chem. 9*, 245−253.
(41) Stanton, B. Z., Peng, L. F., Maloof, N., Nakai, K., Wang, X., Duffner, J. L., Taveras, K. M., Hyman, J. M., Lee, S. W., Koehler, A. N., Chen, J. K., Fox, J. L., Mandinova, A., and Schreiber, S. L. (2009) A

DOI: 10.1021/acschembio.5b00577
ACS Chem. Biol. 2016, 11, 139−148

small molecule that binds Hedgehog and blocks its signaling in human cells. *Nat. Chem. Biol. 5*, 154−156.
(42) Vegas, A. J., Bradner, J. E., Tang, W. P., McPherson, O. M., Greenberg, E. F., Koehler, A. N., and Schreiber, S. L. (2007) Fluorous-based small-molecule microarrays for the discovery of histone deacetylase inhibitors. *Angew. Chem., Int. Ed. 46*, 7960−7964.
(43) Sztuba-Solinska, J., Shenoy, S. R., Gareiss, P., Krumpe, L. R., Le Grice, S. F., O'Keefe, B. R., and Schneekloth, J. S., Jr. (2014) Identification of biologically active, HIV TAR RNA-binding small molecules using small molecule microarrays. *J. Am. Chem. Soc. 136*, 8402−8410.
(44) Carter, M. E., and Brunet, A. (2007) FOXO transcription factors. *Curr. Biol. 17*, R113−114.
(45) Michlewski, G., and Krzyzosiak, W. J. (2004) Molecular architecture of CAG repeats in human disease related transcripts. *J. Mol. Biol. 340*, 665−679.
(46) Mathad, R. I., Hatzakis, E., Dai, J., and Yang, D. (2011) c-MYC promoter G-quadruplex formed at the 5′-end of NHE III1 element: insights into biological relevance and parallel-stranded G-quadruplex stability. *Nucleic Acids Res. 39*, 9023−9033.
(47) Murat, P., Singh, Y., and Defrancq, E. (2011) Methods for investigating G-quadruplex DNA/ligand interactions. *Chem. Soc. Rev. 40*, 5293−5307.
(48) De Crescenzo, G., Boucher, C., Durocher, Y., and Jolicoeur, M. (2008) Kinetic Characterization by Surface Plasmon Resonance-Based Biosensors: Principle and Emerging Trends. *Cell. Mol. Bioeng. 1*, 204−215.
(49) Lemarteleur, T., Gomez, D., Paterski, R., Mandine, E., Mailliet, P., and Riou, J. F. (2004) Stabilization of the c-myc gene promoter quadruplex by specific ligands' inhibitors of telomerase. *Biochem. Biophys. Res. Commun. 323*, 802−808.
(50) Ou, T. M., Lu, Y. J., Zhang, C., Huang, Z. S., Wang, X. D., Tan, J. H., Chen, Y., Ma, D. L., Wong, K. Y., Tang, J. C., Chan, A. S., and Gu, L. Q. (2007) Stabilization of G-quadruplex DNA and down-regulation of oncogene c-myc by quindoline derivatives. *J. Med. Chem. 50*, 1465−1474.
(51) Brown, R. V., Danford, F. L., Gokhale, V., Hurley, L. H., and Brooks, T. A. (2011) Demonstration that drug-targeted down-regulation of MYC in non-Hodgkins lymphoma is directly mediated through the promoter G-quadruplex. *J. Biol. Chem. 286*, 41018−41027.
(52) Pelicci, P. G., Knowles, D. M., 2nd, Magrath, I., and Dalla-Favera, R. (1986) Chromosomal breakpoints and structural alterations of the c-myc locus differ in endemic and sporadic forms of Burkitt lymphoma. *Proc. Natl. Acad. Sci. U. S. A. 83*, 2984−2988.
(53) Kuehl, W. M., and Bergsagel, P. L. (2012) MYC addiction: a potential therapeutic target in MM. *Blood 120*, 2351−2352.
(54) Shou, Y., Martelli, M. L., Gabrea, A., Qi, Y., Brents, L. A., Roschke, A., Dewald, G., Kirsch, I. R., Bergsagel, P. L., and Kuehl, W. M. (2000) Diverse karyotypic abnormalities of the c-myc locus associated with c-myc dysregulation and tumor progression in multiple myeloma. *Proc. Natl. Acad. Sci. U. S. A. 97*, 228−233.
(55) Thomas, L. R., and Tansey, W. P. (2011) Proteolytic control of the oncoprotein transcription factor Myc. *Adv. Cancer Res. 110*, 77−106.
(56) Geiss, G. K., Bumgarner, R. E., Birditt, B., Dahl, T., Dowidar, N., Dunaway, D. L., Fell, H. P., Ferree, S., George, R. D., Grogan, T., James, J. J., Maysuria, M., Mitton, J. D., Oliveri, P., Osborn, J. L., Peng, T., Ratcliffe, A. L., Webster, P. J., Davidson, E. H., Hood, L., and Dimitrov, K. (2008) Direct multiplexed measurement of gene expression with color-coded probe pairs. *Nat. Biotechnol. 26*, 317−325.
(57) Weinert, E. E., Dondi, R., Colloredo-Melz, S., Frankenfield, K. N., Mitchell, C. H., Freccero, M., and Rokita, S. E. (2006) Substituents on quinone methides strongly modulate formation and stability of their nucleophilic adducts. *J. Am. Chem. Soc. 128*, 11940−11947.
(58) Herzig, Y., Lerman, L., Goldenberg, W., Lerner, D., Gottlieb, H. E., and Nudelman, A. (2006) Hydroxy-1-aminoindans and derivatives: Preparation, stability, and reactivity. *J. Org. Chem. 71*, 4130−4140.
(59) McLean, L. R., Zhang, Y., Li, H., Li, Z. Y., Lukasczyk, U., Choi, Y. M., Han, Z. N., Prisco, J., Fordham, J., Tsay, J. T., Reiling, S., Vaz, R. J., and Li, Y. (2009) Discovery of covalent inhibitors for MIF tautomerase via cocrystal structures with phantom hits from virtual screening. *Bioorg. Med. Chem. Lett. 19*, 6717−6720.
(60) Chambers, V. S., Marsico, G., Boutell, J. M., Di Antonio, M., Smith, G. P., and Balasubramanian, S. (2015) High-throughput sequencing of DNA G-quadruplex structures in the human genome. *Nat. Biotechnol. 33*, 877.
(61) Bradner, J. E., McPherson, O. M., and Koehler, A. N. (2006) A method for the covalent capture and screening of diverse small molecules in a microarray format. *Nat. Protoc 1*, 2344−2352.
(62) Simmons, J. K., Patel, J., Michalowski, A., Zhang, S., Wei, B. R., Sullivan, P., Gamache, B., Felsenstein, K., Kuehl, W. M., Simpson, R. M., Zingone, A., Landgren, O., and Mock, B. A. (2014) TORC1 and class I HDAC inhibitors synergize to suppress mature B cell neoplasms. *Mol. Oncol. 8*, 261−272.
(63) Chen, J. Q., Heldman, M. R., Herrmann, M. A., Kedei, N., Woo, W., Blumberg, P. M., and Goldsmith, P. K. (2013) Absolute quantitation of endogenous proteins with precision and accuracy using a capillary Western system. *Anal. Biochem. 442*, 97−103.

DOI: 10.1021/acschembio.5b00577
ACS Chem. Biol. 2016, 11, 139−148